EPR and theoretical studies of negatively charged carbon vacancy in 4*H*-SiC

T. Umeda, Y. Ishitsuka, and J. Isoya
Research Center for Knowledge Communities, University of Tsukuba, Tsukuba 305-8550, Japan

N. T. Son and E. Janzén
Department of Physics and Measurement Technology, Linköping University, S-581 83 Linköping, Sweden

N. Morishita, T. Ohshima, and H. Itoh
Japan Atomic Energy Research Institute, Takasaki 370-1292, Japan

A. Gali
Department of Atomic Physics, Budapest University of Technology and Economics, Budafoki út 8., H-1111 Budapest, Hungary
(Received 5 October 2004; revised manuscript received 19 November 2004; published 23 May 2005)

Carbon vacancies (V_C) are typical intrinsic defects in silicon carbides (SiC) and so far have been observed only in the form of positively charged states in *p*-type or semi-insulating SiC. Here, we present electron-paramagnetic-resonance (EPR) and photoinduced EPR (photo-EPR) observations of their negatively charged state (V_C^-) in *n*-type 4*H*-SiC. This EPR center (called HEI1) is characterized by an electron spin of 1/2 in a Si-Si antibonding state of V_C. First-principles calculations confirm that the HEI1 center arises from V_C^- at hexagonal sites. The HEI1 spectrum shows a transition between C_{1h} and C_{3v} symmetries due to a fast reorientation effect reflected in the nature of this defect. The photo-EPR data suggest that V_C^{2-} is the dominant form of V_C when the Fermi level lies 1.1 eV below the conduction band.

DOI: 10.1103/PhysRevB.71.193202 PACS number(s): 61.72.Ji, 76.30.Mi, 71.15.−m

Carbon vacancies (V_C) are typical intrinsic defects in radiation (ion, electron, etc.) -damaged or semi-insulating silicon carbides (SiC).[1–6] They remain in as-grown wafers or device structures because of their high thermal stability,[3,4,6] and therefore largely influence the electronic properties of SiC, such as the doping efficiency, semi-insulating mechanism, and carrier transport and lifetime. They are often observed in *p*-type or semi-insulating samples by means of electron paramagnetic resonance (EPR): electron-spin-1/2 centers of EI5 and EI6 in 4*H*-SiC (Refs. 1 and 6) or ID1 and ID2 in semi-insulating 4*H*-SiC,[3] and those of Ky1 to Ky3 in 6*H*-SiC.[5] The EI5 (ID1/Ky1/Ky2) and EI6 (ID2/Ky3) centers have been identified as positively charged carbon vacancies (V_C^+) at quasicubic (*k*) and hexagonal (*h*) sites, respectively,[5–8] and their electronic levels have been studied by photoinduced EPR (photo-EPR).[2] However, their negatively charged state (V_C^-), which should also be EPR active with electron spin $S=1/2$,[9] has not been observed yet. This state is important for evaluating the electronic role of V_C in *n*-type or semi-insulating regions. For example, the gap state of V_C^- will act as a dominant deep trap in *n*-type or semi-insulating regions.

In this paper, we present EPR and photo-EPR data on the V_C^- state in 4*H*-SiC. The *n*-type 4*H*-SiC samples were prepared by high-temperature electron irradiation. In these samples, we found a new EPR center, named HEI1, whose hyperfine (HF) interactions clearly indicate it originates from a type of V_C^-. By comparing the HF parameters with those of first-principles calculations, we conclude that this new center corresponds to V_C^- at the *h* site. The atomic and electronic structures are strikingly different from those of V_C^+, and such a contrast is quite similar to what has earlier been observed for vacancies ($V^\pm$) in silicon.[10] The HEI1 center exhibited a fast reorientation phenomenon due to the nature of V_C^-. In the last part, we show photo-EPR data and evaluate the electronic levels of V_C in the energy gap of 4*H*-SiC (3.26 eV).

The starting samples were prepared from a 1.5-mm-thick nitrogen-doped *n*-type 4*H*-SiC(0001) wafer (room-temperature carrier concentration $\approx 10^{17}$ cm^{-3}) made by Nippon Steel Corporation. The samples were uniformly irradiated by 3.5-MeV electrons with a dose of $(2-4)\times 10^{18}\ e/\mathrm{cm}^2$ at 850 °C. This high-temperature irradiation created V_C dominantly in the samples, which is evidenced by our *p*-type samples with the same irradiation condition.[6] In addition, the 850 °C annealing held the Fermi level above the midgap, which is necessary for detecting V_C^-. EPR measurements were carried out using a Bruker E500 X-band ($\approx$9.452 GHz) spectrometer. In the photo-EPR measurements, we used a single-grating 0.25-m Jobin-Yvone monochromator and a 150-W xenon lamp. The EPR spectrum was measured in decreasing steps of 10 nm in wavelength. In this system, the uncertainty of the excitation energy was reduced to less than ±0.06 eV.[2]

First-principles LSDA-PZ (local spin density functional approximation within the parametrization of Perdew and Zunger[11,12]) calculations were carried out to study the negatively charged carbon vacancies in 4*H*-SiC. We focused our investigation mainly on the resulting geometry and corresponding HF tensors of the defects. We used a 96-atom supercell to model the 4*H*-SiC with a 2^3K Monkhorst-Pack K-point set.[13] We have already shown earlier that this supercell and K-point set provides the convergent geometry and total energy for the positively charged carbon vacancies.[7] The convergent geometry and HF tensors were calculated

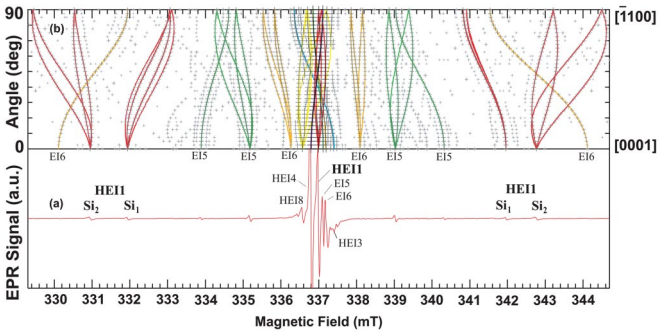

FIG. 1. (Color online) EPR measurements of electron-irradiated *n*-type 4*H*-SiC at 60 K. (a) EPR spectrum for $\mathbf{B}\|[0001]$. (b) Angular dependence of signal positions for **B** rotation in the $(11\bar{2}0)$ plane. Solid lines are simulated angular patterns. For HEI1, the lines were calculated using spin-Hamiltonian Eq. (1) and the parameters in Table I.

using the CP-PAW code, which utilizes the projector augmented-wave method.[14,15] This makes it possible to use a relatively small basis set in the plane-wave expansion (30 Ry in this case) and calculate the HF tensors accurately. During the geometry optimization, all the atoms were allowed to relax until the forces were below 0.5 mhartree/bohr. This method has already been successfully used to calculate the HF tensors of the positively charged carbon vacancies in 4*H*-SiC.[7]

An EPR spectrum of the *n*-type sample at 60 K under room-light illumination is shown in Fig. 1(a). The illumination enhanced the intensities of the EPR signals we want to highlight. In this sample, several new EPR centers appeared, which we name HEI1 to HEI8. Among these centers, HEI1 (electron spin $S=1/2$) shows two strong hyperfine (HF) interactions, denoted by "Si_1" and "Si_2." The intensity ratio of the HEI1 spectrum was 100:5:6 for the central line, Si_1, and Si_2, respectively. This suggests that both HF interactions originate from a ^{29}Si atom (nuclear spin $I=1/2$, natural abundance=4.7%). Namely, an unpaired electron of the HEI1 center distributes on two Si atoms. Such a distribution is well known for a negatively charged vacancy in silicon (V^-, the G2 center), where an unpaired electron is located in the antibonding state of one of two elongated Si-Si bonds in a vacancy.[10] This unpaired electron mainly distributes on two Si atoms of the negatively charged bond, resulting in two strong ^{29}Si HF interactions. This would suggest that the HEI1 center arises from a type of V_C^-, which is confirmed by the following angular dependence data for the EPR spectrum.

The signal positions as a function of the rotation angle of magnetic field (**B**) in the $(11\bar{2}0)$ plane are shown in Fig. 1(b), from which the angular pattern of the HEI1 spectrum (solid lines) can be well described by the Hamiltonian

$$H = \mu_B \mathbf{S}\cdot\mathbf{g}\cdot\mathbf{B} + \mathbf{S}\cdot\mathbf{A}\cdot\mathbf{I} - g_n\beta_n\mathbf{I}\cdot\mathbf{B}, \qquad (1)$$

where μ_B is the Bohr magneton, **g** is a g tensor, **S** is an electron spin operator, **A** is a HF tensor for Si_1 or Si_2, **I** is a nuclear spin operator ($I=1/2$), g_n is the nuclear g value for ^{29}Si (−1.1106), and β_n is the nuclear magneton. The spin-Hamiltonian parameters (**g** and **A**) of HEI1 determined from the fit are shown in Table I. The HF tensors for Si_1 and Si_2 are nearly axially symmetric and can therefore be well examined by a simple LCAO (linear combination of atomic orbitals) analysis of Si's 3*s* and 3*p* orbitals. The directions of the *sp*-hybridized orbitals for Si_1 and Si_2 were determined as shown in Table I or in Fig. 2(a). The two Si atoms are well fitted to one c-axial Si atom (Si_1) and one of three Si atoms in plane (Si_2) of a V_C. Thus, an unpaired electron of HEI1 is believed to be in the antibonding state of the Si_1-Si_2 bond. We should mention that this antibonding orbital is repelled by the Si_1-Si_2 bonding orbital [the bonding orbital can be seen in the EI5 center, Fig. 2(b), where Si_1-Si_2 atomic pair is formed[7]]. This would be a consequence of minimizing the electron repulsion and is thus quite reasonable in our model. The atomic structure shown in Fig. 2(a) has a C_{1h} symmetry with respect to the $(11\bar{2}0)$ plane. This is also consistent with the C_{1h} symmetry of the g tensor for HEI1. Consequently, we conclude that the origin of HEI1 is V_C^-.

TABLE I. Spin-Hamiltonian parameters of HEI1 and calculated HF tensors for *h*-site V_C^-. Principal values of **A** are expressed in mT using the conversion factor that 1 mT=28.02 MHz. θ represents the main (Z) principal direction from the c axis.

	$X(\perp)$	$Y(\perp)$	$Z(\|)$	θ
HEI1 (C_{1h}), 60 K				
g	2.00287	2.00407	2.00459	38°
A(Si_1)	7.76	7.76	10.07	7°
A(Si_2)	11.78	11.67	15.19	101°
HEI1 (C_{3v}), 150 K				
g	2.00381	2.00381	2.00401	0°
A(Si_1)	7.79	7.79	10.04	0°
A(Si_2)	Not observed due to broadening			
h-site V_C^-(C_{1h}), theory				
A(Si_1)	7.78	7.78	10.03	7°
A(Si_2)	11.24	11.24	14.45	101°
A($Si_{3,4}$)	0.14	0.25	0.32	

From the LCAO analysis,[1,6,7,10] we estimated the distributions of an unpaired electron (η^2) on Si_1 and Si_2 to be 24.1% and 36.6%, respectively [Fig. 2(a)]. The η^2 values were cal-

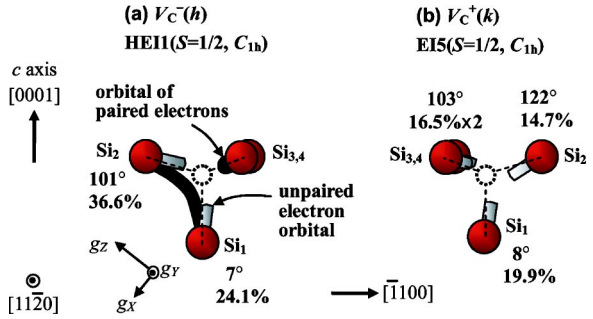

FIG. 2. (Color online) Atomic models (a) for V_C^- (HEI1) and (b) for V_C^+ (EI5).[7] For unpaired-electron orbitals on each Si atom, the direction (θ) and distribution (η^2) are given in the figure.

culated by the sum of 3*s*- and 3*p*-orbital densities, $\eta^2\alpha^2 + \eta^2\beta^2$, where $\eta^2\alpha^2 = A_{\rm iso}({\rm mT})/163.93$, $\eta^2\beta^2 = A_{\rm aniso}({\rm mT})/4.08$, $A_{\rm iso} = (A_{\parallel} + 2A_{\perp})/3$, $A_{\rm aniso} = (A_{\parallel} - A_{\perp})/3$, and $\alpha^2 + \beta^2 = 1$.[16] One may assume that the Si_1 or Si_2 HF structure originates from three to six ^{13}C atoms ($I = 1/2$, natural abundance = 1.1%), which would make the intensity ratio of the Si_1 or Si_2 HF structure about 4.7% (=ideal intensity ratio for a ^{29}Si HF interaction). In this case, however, the η^2 values were calculated to be 26.4% or 40.0% for *each* C atom using the atomic coefficients of carbon [$\eta^2\alpha^2 = A_{\rm iso}({\rm mT})/134.77$ for 2*s*-orbital, $\eta^2\beta^2 = A_{\rm aniso}({\rm mT})/3.83$ for 2*p*-orbital].[16] Thus, the total distribution was much larger than 100%. Therefore, we can conclude again that the Si_1 and Si_2 HF structures are due to ^{29}Si.

It is worth noting that there is a close similarity between $V^{\pm}$ in Si and $V_C^{\pm}$ in SiC. For V^- (G2), an unpaired electron distributes on two Si atoms by 26.5% × 2 (totally 53%) and for V^+ (the G1 center) the distribution is divided among four Si atoms by 14.5% × 4 (totally 58%).[10] From Figs. 2(a) and 2(b), we can see the same trend in V_C^- (HEI1) and V_C^+ (EI5), although the lower crystal symmetry of 4*H*-SiC breaks the equality of Si_{1-4} and causes some deviations from the case of silicon. Since both the $V^{\pm}$ state and the $V_C^{\pm}$ state consist of a combination of Si dangling-bond orbitals, such a similarity can naturally be expected.[17] However, it is interesting that the wave functions of the $V^{\pm}$ and $V_C^{\pm}$ states were found to be quantitatively close, despite their energetic positions in the gap being completely different.[9,10]

In Table I, we compare the measured HF tensors with the calculated ones for V_C^- at the *h* site. The first-principles calculations revealed that *h* and *k* sites cause completely different behaviors in V_C^-. At *h* sites, Jahn-Teller distortion makes a Si_3-Si_4 bond and an unpaired electron distributes on the Si_1-Si_2 side, which is consistent with what we observed in the HEI1 center. At *k* sites, however, an unpaired electron is located in the Si_3-Si_4 side, and hence there should appear another EPR center with quite different angular dependence of the HF satellites. The obtained geometry of V_C^- at both sites agrees very well with the results of an earlier calculation by Zywietz *et al.*,[9] e.g., at *h* sites, the bond lengths are 2.5 Å for Si_3-Si_4 and 2.9 Å for Si_1-Si_2, which are very close to Zywietz's values of 2.6 Å and 2.9 Å, respectively. Here, we compare *h*-site V_C^- with HEI1. (Further details of the results of the calculations will be reported elsewhere.) As is seen in the table, perfect agreement between the HEI1 center and *h*-site V_C^- is obtained in both the principal values and the directions of the HF tensors. Therefore, we conclude that the HEI1 center originates from V_C^- at the *h* site. The reason we could not observe *k*-site V_C^- is still unclear. However, we speculate that this may be related to dynamic reorientation effects, because such a dynamics was clearly observed in the HEI1 center.

The HEI1 spectrum exhibits a thermal-reorientation phenomenon, as shown in Figs. 3(a) and 3(b). As the temperature was raised, the Si_2 HF structure broadened and it eventually disappeared 70 K [Fig. 3(a)]. Simultaneously, the Si_1 HF structure is averaged into a single line [Fig. 3(b)], when the magnetic field is aligned at off-angles ($\neq 0°$). Above 70 K, the HEI1 spectrum showed a simple C_{3v} symmetry

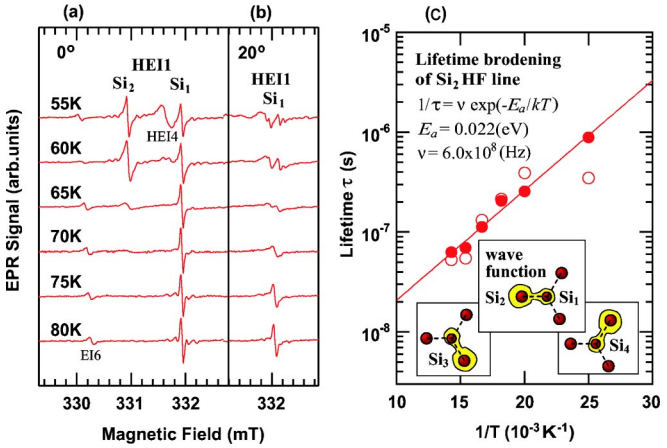

FIG. 3. (Color online) Thermally activated reorientation effect of V_C^-. (a) EPR spectra just for 0° (**B**∥c) show the motional narrowing of the Si_1 HF line but the lifetime broadening of the Si_2 HF line. (b) Off-angle (20°) spectra demonstrate that the Si_1 HF structure is averaged into a single line due to the motional narrowing effect. (c) Temperature dependence of the reorientation lifetime estimated by the lifetime broadening of the Si_2 HF structure. Solid and open circles were obtained for high-field- and low-field-side Si_2 HF lines. The insets schematically show the reorientation of the defect in the (0001) plane.

(see Table I).[18] This transition can be explained by the thermal reorientation of the defect. For HEI1, an unpaired electron is located in one of three equivalent bonds, Si_1-Si_2, Si_1-Si_3, and Si_1-Si_4 [see the inset of Fig. 3(c)]. Thus, the unpaired electron can hop among these three states by thermal activation. Since $Si_{2,3,4}$ atoms are C_{3v}-symmetry related, the thermal-averaging limit also exhibits a C_{3v} symmetry. During the reorientation, the unpaired electron always stays on Si_1 but fully jumps among $Si_{2,3,4}$. Therefore, only the Si_2 HF structure is strongly affected by the lifetime broadening, which is determined by the reorientation speed. Figure 3(c) shows the temperature dependence of reorientation lifetime (τ), which was deduced from the inverse of the lifetime broadening width ($1/\Delta\omega$)[7] for the Si_2 HF structure. We calculated $\Delta\omega$ from $\hbar\Delta\omega = g\mu_B\Delta B$, where ΔB is the half width at half maximum of the Si_2 HF line (in absorption shape) subtracted by the static width (0.30 mT). The static width was measured at 20–40 K. The temperature dependence seems to indicate the thermally activated behavior. The activation energy was roughly estimated to be 0.02 eV. A similar thermally activated reorientation has been observed for EI5, in which three equivalent C_{1h} structures were averaged into a C_{3v} structure with an activation energy of 0.015 eV.[6,7] In that case, however, the disappearance of particular HF structure(s) was not observed,[6,7] because the unpaired electron always stayed on four Si atoms (Si_{1-4}) of V_C [Fig. 2(b)]. The reorientation effects are thus closely related in the nature of these defects. By analogy with the "missing" HF structure of the HEI1 center, the same behavior is also expected for Si_3 and Si_4 HF structures of *k*-site V_C^-. This may be related to the reason we could not observe *k*-site V_C^-.

We also carried out photo-EPR measurements at 77 K to

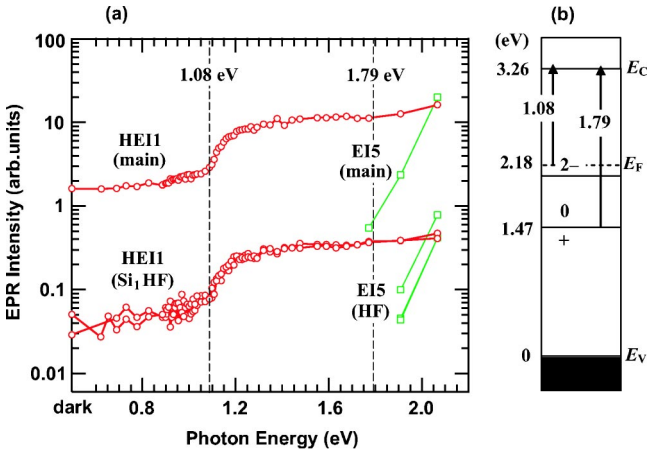

FIG. 4. (Color online) (a) Photo-EPR measurement on HEI1 (V_C^-) and EI5 (V_C^+) at 77 K. EPR intensities shown here were simply taken by peak heights of the first derivative signals. (b) An electronic energy diagram of V_C.

estimate the energy position of V_C^-. The changes in EPR intensities of the central line ("main") and HF lines ("HF") for HEI1 and EI5 are shown in Fig. 4(a). For both centers, the "main" and "HF" curves showed the same behavior, demonstrating that there was no interference from the other signals. Without illumination, only V_C^- (HEI1) and other HEI centers were observed; V_C^+ (EI5 and EI6) was completely absent. This is reasonable for our *n*-type sample. With 1.1-eV light excitation, all EPR signals increased or decreased simultaneously, because it became possible to excite electrons from levels at the Fermi level (E_F) to the conduction band, which caused different charge states for the EPR centers. This excitation increased the HEI1 signal drastically, indicating that $V_C^- + e^-$ (conduction band) was generated from V_C^{2-}. Namely, most of the V_C were converted to V_C^{2-}, when E_F was located at E_C (conduction-band bottom) −1.1 eV. This suggests that the $(-/2-)$ level is located below E_C −1.1 eV or E_V+2.2 eV. Alternatively, another explanation would be that V_C^{2-} is slightly more stable than V_C^- (the so-called weak negative-*U* behavior), and hence V_C^{2-} became dominant in the dark. In fact, the present calculations predicted $U=-0.33$ eV for *h*-site V_C^-. In the previous calculation,[9] *U* was also negative for both *h*-site and *k*-site V_C^- (−0.29 eV). However, we have to note that the total energy of the charged defect represents a problem in the supercell approach. Since the appropriate charge correction for a defect in a solid is still being debated in the literature,[19–21] the negative-*U* property for V_C^- is not yet proven entirely by theory.[22] When we further increased the photon energy to 1.8–1.9 eV, the EI5 signal (V_C^+) became detectable. This indicates that the $(+/0)$ level of V_C is located below E_C −1.8 eV or E_V (valence-band top) +1.5 eV, which is in agreement with the previous work (E_V+1.47 eV).[2] Figure 4(b) summarizes these results.

In summary, we have reported EPR measurements of a negatively charged state of carbon vacancies (V_C^-) in 4*H*-SiC. We found an EPR center, HEI1, and its ^{29}Si HF interactions were well described by an unpaired electron ($S=1/2$) in the antibonding state of Si_1 and Si_2 of V_C. First-principles calculations showed that the HEI1 center corresponds to *h*-site V_C^-. It is worth noting that there is a close similarity between V_C^-(HEI1)/V_C^+(EI5) and V^-(G1)/V^+(G2) in silicon. Photo-EPR measurements suggested that V_C^{2-} becomes dominant when $E_F=E_C-1.1$ eV. The HEI1 spectrum revealed a thermally activated reorientation effect, in which the reorientation caused the lifetime broadening of a particular HF structure (Si_2), resulting in a missing HF structure in the thermally averaging limit.

[1] N. T. Son, P. N. Hai, and E. Janzén, Phys. Rev. B **63**, 201201(R) (2001).
[2] N. T. Son, B. Magnusson, and E. Janzén, Appl. Phys. Lett. **81**, 3945 (2002).
[3] V. V. Konovalov, M. E. Zvanut, and J. van Tol, Phys. Rev. B **68**, 012102 (2003).
[4] N. T. Son, B. Magnusson, Z. Zolnai, A. Ellison, and E. Janzén, Mater. Sci. Forum **457–460**, 437 (2003).
[5] V. Ya. Bratus, T. T. Petrenko, S. M. Okulov, and T. T. Petrenko, Phys. Rev. B **71**, 125202 (2005).
[6] T. Umeda, J. Isoya, N. Morishita, T. Ohshima, and T. Kamiya, Phys. Rev. B **69**, 121201(R) (2004).
[7] T. Umeda, J. Isoya, N. Morishita, T. Ohshima, T. Kamiya, A. Gali, P. Deák, N. T. Son, and E. Janzén, Phys. Rev. B **70**, 235212 (2004); Table I of this paper included a misprint. For "EI6 (C_{3v}) at 5 K, our EPR," the correct **g** parameters are $g_X=g_Y=2.0052$ and $g_Z=2.0026$.
[8] M. Bockstedte, M. Heid, and O. Pankratov, Phys. Rev. B **67**, 193102 (2003).
[9] A. Zywietz, J. Furthmüller, and F. Bechstedt, Phys. Rev. B **59**, 15166 (1999).
[10] G. D. Watkins, *Radiation Damages in Semiconductors* (Dunod, Paris, 1965), p. 97.
[11] W. Kohn and L. J. Sham, Phys. Rev. **140**, A1133 (1965).
[12] J. P. Perdew and A. Zunger, Phys. Rev. B **23**, 5048 (1981).
[13] H. J. Monkhorst and J. D. Pack, Phys. Rev. B **13**, 5188 (1976).
[14] P. E. Blöchl, Phys. Rev. B **50**, 17953 (1994).
[15] P. E. Blöchl, C. J. Först, and J. Schimpl, Bull. Mater. Sci. **26**, p. 33 (2003).
[16] J. A. Weil, J. R. Bolton, and J. E. Wertz, in *Electron Paramagnetic Resonance* (Wiley, New York, 1994).
[17] A. Zywietz, J. Furthmüller, and F. Bechstedt, Phys. Status Solidi B **210**, 13 (1998).
[18] T. Umeda, Y. Ishitsuka, J. Isoya, N. Morishita, T. Ohshima, and T. Kamiya, Mater. Sci. Forum **457–460**, 465 (2004).
[19] G. Makov and M. C. Payne, Phys. Rev. B **51**, 4014 (1995).
[20] U. Gerstmann, P. Deák, R. Rurali, B. Aradi, Th. Frauenheim, and H. Overhof, Physica B **340–342**, 190 (2003).
[21] D. Segev and S.-H. Wei, Phys. Rev. Lett. **91**, 126406 (2003).
[22] Using the Makov-Payne charge correction,[19] *U* was calculated to be +0.07 eV.